MedCrave
Step into the World of Research
Journal of Applied Biotechnology and Bioengineering

Research Article
Open Access
CrossMark

Analyzing the impact of Wi-Fi radiation on structured water stability: a six-phase study with SPIRO field application

Abstract

Objective: This study investigates the capacity of the SPIRO field to structure and preserve the molecular coherence of water exposed to continuous radiofrequency (RF) electromagnetic radiation (EMR) from a Wi-Fi 6 source. The research evaluates whether SPIRO-structured water can resist dielectric and entropic degradation, potentially sustaining its super-coherent phase in near-field artificially polarized EMFs (HF / LF).

Design: A six-phase experimental protocol was implemented using controlled EMR exposure from a 2.4 GHz Wi-Fi 6 router. SPIRO material filtering power 6.3 (P 6.3) and SPIRO material filtering power 31.6 (P 31.6) devices were sequentially applied and withdrawn to evaluate their impact on the structural stability of water over time.

Methods: Quantitative measurements of EMF intensity were recorded using frequency-selective radiofrequency meters. Gas Discharge Visualization (GDV) bioelectrography was employed to monitor changes in entropy, area, intensity, and energy emission of the water sample throughout the protocol. A red/infrared light stimulus was introduced in the final phase to examine synergistic effects with SPIRO structuring.

Sample: A single-source tap water sample was used continuously across all six experimental phases to ensure baseline uniformity and eliminate inter-sample variability. The sample remained under uninterrupted exposure to near-field emissions from a Wi-Fi router throughout the entire protocol, maintaining a consistent and high-intensity EMF stimulus representative of an extreme environmental stressor.

Outcome measures: Primary indicators included GDV-derived measurements of entropy and energy, reflecting the water's capacity to maintain coherent domains, as theorized in quantum electrodynamics (QED) models and exclusion zone (EZ) water literature.

Results: The SPIRO material filtering power 6.3 (P 6.3) induced a measurable structuring effect; however, coherence diminished upon device removal under persistent RF exposure. The SPIRO material filtering power 31.6 (P 31.6) generated a higher-order super-coherent state, maintaining stability over extended EMF exposure. The addition of red/infrared light further enhanced energy absorption without coherence degradation.

Conclusion: Findings support that SPIRO material filtering power 31.6 (P 31.6) promotes a super-coherent water state resilient to RF-induced dielectric perturbation, consistent with models of long-range electromagnetic ordering and coherent domain preservation. This suggests potential applications in biomedical, environmental, and residential settings where water stability under EMF exposure is critical.

Keywords: SPIRO technology, structured water, super-coherence, electromagnetic radiation, Wi-Fi exposure, GDV bioelectrography, dielectric resilience, quantum coherence domains

Volume 12 Issue 4 - 2025

Machado J Joaquín
Electromagnetic Radiation Researcher, EFEIA Institute, USA

Correspondence: Machado J Joaquín, Electromagnetic Radiation Researcher, EFEIA Institute, Miami, Florida, USA

Received: July 21, 2025 | **Published:** August 11, 2025

Introduction

The structuring of water into coherent molecular configurations has gained scientific attention for its relevance to biological integrity, particularly in the form known as exclusion zone (EZ) water. Characterized by an organized hydrogen-bond network adjacent to hydrophilic surfaces, EZ water supports cellular stability, hydration layers, and redox regulation. Research by Pollack and colleagues highlights this structured phase's role in sustaining intracellular order and mitigating oxidative stress. However, the integrity of such water structures is notably vulnerable to anthropogenic electromagnetic fields (EMFs), particularly polarized radiofrequency (RF) emissions such as those produced by Wi-Fi routers. These fields may interfere with dipole alignment and hydrogen bonding, undermining the stability of structured water essential to physiological function.

In response, several theoretical and experimental frameworks have sought to explain and preserve water's coherence under EMF stress. Among them, the quantum electrodynamics (QED) model developed by Del Giudice and Preparata proposes that water can form long-range coherent domains (CDs) when exposed to weak, coherent electromagnetic fields. Such domains are hypothesized to resist entropy increase by aligning molecular oscillations in phase. More recently, Messori[1] expanded on this concept, providing empirical support for the existence of a "super-coherent" water phase—resilient to electromagnetic disruption and capable of maintaining order in energetically hostile environments.

SPIRO (Spin Radiation Organizer) technology has emerged as a passive EMF modulation system that aligns conceptually with these coherence models. Based on nanocomposite films embedded

with magnetic nanoparticles, SPIRO interacts with incident EMFs by influencing spin alignment and polarization behavior rather than blocking amplitude. This creates a localized, low-intensity coherent field environment that may foster or sustain molecular order in adjacent systems. Two models of this technology—SPIRO material filtering power 6.3 (P 6.3) and SPIRO material filtering power 31.6 (P 31.6)—offer varying levels of field density and coherence support.

This study aims to evaluate whether water structured using SPIRO technology can maintain coherence when subjected to continuous near-field Wi-Fi radiation. Previous studies have assessed SPIRO's ability to initiate structuring; this investigation extends the inquiry by examining post-exposure persistence. Using gas discharge visualization (GDV) analysis over a six-phase protocol, the research probes both the immediate and residual coherence effects induced by SPIRO, with implications for EMF mitigation in biological and environmental systems.

Background & Rationale

The interaction between water and electromagnetic radiation has long been recognized as a determinant of water's structural state, especially at microwave and radiofrequency (RF) frequencies. Man-made electromagnetic fields (EMFs), particularly those emitted by Wi-Fi systems operating at 2.4 GHz, produce linearly polarized radiation that induces dielectric relaxation and rotational excitation in water molecules.[2,3] These interactions disrupt hydrogen bonding networks and destabilize exclusion zone (EZ) water, compromising its biological function. Fesenko et al.,[4] further demonstrated RF-induced alterations in water's electrochemical behavior, adding to concerns about EMF-induced decoherence in structured water environments.

While most EMF shielding strategies focus on reducing exposure amplitude, recent quantum electrodynamics (QED) models suggest that water's vulnerability to EMF lies more in polarization asymmetry than in field strength itself. According to the theoretical framework proposed by Del Giudice and Preparata, coherent water domains stabilized by zero-point field interactions can resist entropic degradation only when phase alignment is actively maintained. Supporting this, Messori[1] provided experimental evidence that water can enter a "super-coherent" state, resilient to EMF disruption, provided it is supported by a reinforcing field source that preserves molecular synchrony.

This conceptual framework aligns with the operational principle of SPIRO technology, a passive EMF modulation system based on nanocomposites containing magnetic nanoparticles. Unlike traditional shielding devices, SPIRO does not block or absorb electromagnetic fields, but interacts with them by modulating their spin and polarization symmetry, thereby creating a coherent field environment around the treated system. Two variants of this technology are tested in this study: SPIRO P 6.3, a lower-density model, and SPIRO P 31.6, a higher-density version. Rather than merely initiating structured states, these devices are hypothesized to stabilize them, particularly through the induction of a durable super-coherent phase capable of persisting even after the source device is removed.

Additional theoretical support comes from Zadeh-Haghighi and Simon,[5] who describe the radical pair mechanism—a quantum biological process whereby weak magnetic fields stabilize spin-correlated molecular pairs. This may offer a field-based explanation for the observed resilience of SPIRO-treated water to EMF-induced decoherence and oxidative degradation.

These considerations motivate the design of the present six-phase experiment, which aims not only to evaluate the structuring capacity of SPIRO devices but also to test the persistence of such structuring in the face of continuous Wi-Fi radiation. Specifically, the study investigates whether the water coherence induced by SPIRO P 6.3 and P 31.6 is maintained after the devices are removed, and how this effect is modulated by additional red and infrared light exposure.

It is hypothesized that water samples treated with SPIRO P 31.6 will demonstrate significantly higher retention of structural coherence—measured via gas discharge visualization (GDV) indicators such as area, energy, and intensity—under and after exposure to Wi-Fi, in comparison to both untreated controls and samples treated with SPIRO P 6.3. By focusing on coherence persistence rather than initiation, the study addresses a critical gap in EMF mitigation research relevant to biological and environmental systems. Its findings may inform emerging technologies for sustaining molecular order in fields ranging from biophysics and environmental health to materials science and water treatment.

Methodology

Experimental design: six-phase structure

Phase	Duration	SPIRO application	Exposure conditions	Purpose
1. Baseline – No Device	21h 39m	None	Continuous Wi-Fi	Establish baseline coherence metrics under EMF stress without SPIRO structuring.
2. SPIRO P 6.3 Application	23h 49m	SPIRO P 6.3	Continuous Wi-Fi	Observe induction of molecular coherence from a standard SPIRO field.
3. Post-SPIRO P 6.3 Monitoring	24h 10m	Removed	Continuous Wi-Fi	Evaluate the persistence of water structure after removing SPIRO P 6.3.
4. SPIRO P 31.6 Application	23h 58m	SPIRO P 31.6	Continuous Wi-Fi	Assess super-coherent state induction via enhanced SPIRO structuring.
5. Post-SPIRO P 31.6 Monitoring	26h 56m	Removed	Continuous Wi-Fi	Examine long-term structural integrity after SPIRO P 31.6 removal.
6. Infrared Light Synergy	8h 48m	None (Post-SPIRO structured water)	Wi-Fi + Red/NIR Light	Test cumulative effects of light energy on SPIRO-induced structured water.

Citation: Joaquín MJ. Analyzing the impact of Wi-Fi radiation on structured water stability: a six-phase study with SPIRO field application. *J Appl Biotechnol Bioeng* . 2025;12(4):159–166. DOI: 10.15406/jabb.2025.12.00398

This study employed a six-phase longitudinal protocol to evaluate the ability of SPIRO technology to induce and sustain structured water under continuous electromagnetic field (EMF) exposure from a Wi-Fi 6 router. The experimental protocol ran from January 29 to February 3, 2024, using a single batch of tap water maintained under controlled environmental conditions to eliminate inter-sample variability. The aim was to simulate prolonged near-field EMF exposure while monitoring coherence shifts in water's structure in real time.

A NETGEAR Wi-Fi 6 router operating at 2.4 GHz served as the EMF source. EM field intensities were tracked using frequency-selective RF meters calibrated for high temporal resolution. Water structuring was evaluated across six sequential phases, each lasting between 8 and 27 hours, with real-time bioelectrographic tracking via gas discharge visualization (GDV) technology. SPIRO P 6.3 and SPIRO P 31.6 devices were introduced and withdrawn at specific intervals to observe both induction and persistence of coherence.

Phase descriptions

Phase 1 (Baseline – No device): An untreated water sample was exposed to continuous Wi-Fi EMF for 21 hours and 39 minutes without SPIRO intervention. GDV metrics (entropy, area, intensity, energy) were recorded to establish the baseline profile of water exposed to EMF without structural mitigation.

Phase 2 (SPIRO P 6.3 application): A standard piece of SPIRO P 6.3 was placed adjacent to the water sample for 23 hours and 49 minutes. Bioelectrographic parameters were monitored to assess initial coherence induction and molecular reorganization attributed to the SPIRO field.

Phase 3 (Post-SPIRO P 6.3 monitoring): The SPIRO P 6.3 was removed, and coherence metrics were tracked for 24 hours and 10 minutes to determine structural resilience in the absence of ongoing SPIRO exposure.

Phase 4 (SPIRO P 31.6 application): The higher-density SPIRO P 31.6 was introduced for 23 hours and 58 minutes. This phase aimed to determine whether the Ultra model could achieve a super-coherent state characterized by elevated and stable GDV coherence indicators.

Phase 5 (Post-SPIRO P 31.6 monitoring): The device was removed, and the sample was monitored for 26 hours and 56 minutes to assess long-term structural integrity post-induction. Special attention was given to identifying persistent or delayed structural decay patterns.

Phase 6 (Infrared light synergy): To explore cumulative and synergistic effects, the water—now previously structured with SPIRO P 31.6—was subjected to an 8-hour and 48-minute stimulus involving

Citation: Joaquín MJ. Analyzing the impact of Wi-Fi radiation on structured water stability: a six-phase study with SPIRO field application. *J Appl Biotechnol Bioeng* . 2025;12(4):159–166. DOI: 10.15406/jabb.2025.12.00398

combined Wi-Fi and near-infrared (NIR) light exposure. This phase evaluated whether red/NIR light could reinforce or destabilize existing structured states.

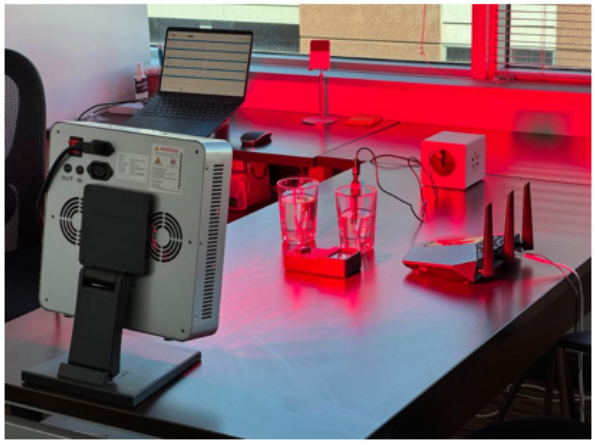

Instrumentation and measurement

Water samples: Four vessels were filled simultaneously with water from the same municipal source to ensure chemical homogeneity. Each sample was used for an independent yet parallel testing condition across the six experimental phases. Rather than relying on isolated spot measurements, bioelectrographic recording was continuous throughout each phase, capturing real-time fluctuations in water structuring parameters under different field conditions. Technical replicability was not dependent on multiple biological replicates but ensured through strict adherence to GDV calibration protocols and by applying uniform acquisition settings across all measurements. This methodological consistency enables reproducible coherence tracking over time while avoiding confounds associated with sequential exposure or sample memory effects.

Gas discharge visualization (GDV) Camera: The GDV camera captured bioelectrographic data across all six phases, focusing on key parameters—entropy, area, intensity, and energy levels—within the water's molecular structure. These parameters served as proxies for structural coherence, enabling real-time detection of changes as SPIRO devices were applied and removed. To ensure methodological consistency, image acquisition was calibrated to maintain a stable saturation range between 5,000 and 7,000 pixels, the ideal operational window for valid GDV signal interpretation. This saturation threshold ensured optimal signal-to-noise ratio and reproducibility, allowing all area-based coherence metrics to be interpreted within standardized GDV evaluation parameters.

Electromagnetic field measurement equipment: A comprehensive suite of electromagnetic measurement instruments was employed to characterize the exposure environment. Wi-Fi meters, gaussmeters, electrical field meters, EMI meters, and frequency-selective RF meters measured the power density and field characteristics of the Wi-Fi signal from the NETGEAR router, recording electric and magnetic fields across multiple frequency ranges. Measured electromagnetic exposure levels included:

- 705.000 mW/m² maximum radiated power received in Sub6 Band
- 78 mW/m² pulses average received of Wi-Fi frequencies
- 710 µG (microGauss) for ELF and VLF ranges (13 Hz - 75 KHz)
- LF measurements showing peaks of 61.600 microGauss with an average of 48.400 microGauss
- and LF/ELF electrical fields with peaks of 91 V/m and an average of 64 V/m.

In Phase 6, the measurement equipment also captured irradiance from the additional red and infrared light sources to assess the combined EMF effects on water structuring. The use of multiple specialized meters ensured comprehensive electromagnetic characterization across the experimental phases.

Additional measurements: PH levels were recorded throughout the study to control for environmental influences. Additionally, near-field EMF effects from the router were continuously monitored to evaluate background EMF impact on water structuring. These supplementary measurements helped account for external variables that might affect water's structural coherence.

Relevant environmental factors

During the execution of the six-phase experiment, various environmental factors were identified that, while not compromising the validity of the experimental design, should be considered when interpreting results and defining future methodological improvements.

1. Presence of uncontrolled neighboring Wi-Fi signals: The urban laboratory environment inevitably involved reception of Wi-Fi signals from neighboring offices, which fluctuated dynamically based on data traffic during day and night periods. However, these sources are classified as far-field, and their radiated power was quantitatively negligible compared to the reactive near-field exposure deliberately applied from the experimental Wi-Fi router. Therefore, these external signals should be considered as an uncontrolled but non-significant environmental variable for the study's purposes.

2. Partial natural lighting conditions: The experimental enclosure was maintained without artificial lighting, allowing only natural light entry through a window covered with solar control film and UV filter. This configuration generated a controlled daytime penumbra environment, with average illumination levels between 600 and 800 lux, and <10 lux during nighttime. This condition allowed indirect evaluation of the role of ambient lighting in water molecular structuring dynamics, especially under electromagnetic exposure.

3. Stable ambient temperature: A constant temperature of approximately 21.9°C was maintained throughout the entire evaluation week. This thermal stability helped minimize any bias from external energetic variations that could alter the dielectric properties or water structure.[6–9]

4. Main electromagnetic pulse stability: Although the study did not include dynamic in-situ monitoring of complete spectra, a continuous observation methodology was implemented using an environmental bioelectrography camera with programmed 3-second captures and specialized microwave radiofrequency meters. These instruments, operated in conjunction with the ENVIONIC recording system, allowed obtaining frequency-selective spectral traces. Results showed a dominant and stable Wi-Fi signal, without anomalous peaks or unexpected modulations, thus validating the consistency of the electromagnetic exposure environment throughout the study.

5. Harmonic interference and electrical grid transients (dirty electricity): The presence of high-frequency signals and irregular peaks known as "dirty electricity" was identified, originating from harmonics and transients circulating in the building's electrical

grid. These interferences were detected through exploratory measurements with an Emitter meter, recording an average of 800 millivolts additional above the base threshold. However, this monitoring was not performed continuously or systematically, and the sources of these emissions were distant from the water samples, not representing near-field exposure. Given that the experimental protocol focused exclusively on controlled reactive near-field exposure generated by the Wi-Fi router—the only emitting source located in proximity to the samples—dirty electricity is considered an environmental variable present but not significant within the study framework.

6. Water resource homogeneity: All samples used were extracted from the building's potable water system. Previous exploratory tests with high and low mineralization waters showed similar structural behaviors when exposed to SPIRO action, which justifies the choice of this resource and reinforces the reproducibility of findings independent of base mineralization.

Results

General results overview

Phase	Observed GDV Parameter Shifts	Coherence Dynamics	Interpretative Inference
1 (Baseline)	**Area:** 5,315-6,408 pixels (median: 5,949.6); Energy: 1.4-2.2 ×10^-2 J (median: 2.0); **Intensity:** 66.0-89.3 R.U. (median: 82.1); Moderate entropy dispersal	Absence of coherent structuring under EMF stress; baseline molecular disorganization	Disordered state consistent with non-coherent dipole oscillation under Wi-Fi EMF exposure
2 (SPIRO P 6.3)	**Reduced stabilized area:** 5,400-5,800 pixels; **Energy decline:** 1.5-1.6 ×10^-2 J; Lowered entropy and deviation (33.9-196.1 pixels, median: 97.3)	Induction of compact, short-range molecular coherence; condensed molecular distribution	Formation of localized coherent domains; dipolar phase alignment under SPIRO field modulation creating stable, lower-entropy state
3 (Post-P 6.3)	Entropy increase to 174.3 maximum; Scattered distribution patterns; Area deviation fluctuations over 24 hours	Gradual decoherence post-device removal; structural vulnerability without field support	Partial memory effect with limited resilience; molecular organization susceptible to prolonged EMF exposure without sustained external intervention
4 (SPIRO P 31.6)	**Increased area:** 5,876-7,096 pixels (median: 6,317.9); **Enhanced energy:** 1.9-2.7 ×10^-2 J (median: 2.1); **Elevated intensity:** 79.0-95.0 R.U. (median: 84.9)	High-order, stable coherence across expanded spatial matrix; super-coherent state emergence	Onset of super-coherent domain formation per QED phase-locking hypothesis; robust molecular alignment without system destabilization
5 (Post-P 31.6)	**Sustained area:** 5,843-6,686 pixels (median: 6,169.16); **Stable energy:** 1.91-2.34 ×10^-2 J (median: 2.14); **Consistent intensity:** 78.66-90.39 R.U. (median: 84.76) over 27 hours	Maintenance of induced super-coherence; no significant parameter decay	Long-range phase stabilization; delayed decoherence consistent with durable field-induced order and enhanced EMF resilience
6 (Wi-Fi + Infrared)	**Enhanced energy:** 2.04-2.49 ×10^-2 J (median: 2.30); **Stable area:** 6,106-6,993 pixels (median: 6,520.31); **Maintained intensity:** 79.37-93.78 R.U. (median: 88.62)	Photonic energy absorption without structural destabilization; coherence amplification under combined stimuli	Coherence enhancement via resonant coupling; synergistic reinforcement of ordered water domains through constructive electromagnetic-photonic interaction

Graphical analysis observations

Visual and quantitative GDV data across the six experimental phases reveal distinct shifts in water's structural coherence as influenced by the presence, removal, and type of SPIRO device applied. The parameters monitored—area, energy emission, entropy, and intensity—serve as proxies for the degree of molecular order and structural stability under EMF exposure.[10–15]

Area and energy emission dynamics

Area and Energy Emission Dynamics

Phase 1 (Baseline - Water Glass in Front of WiFi Router): Baseline measurements established initial parameters with area readings of 5,315-6,408 pixels (median: 5,949.6), energy emission of 1.4-2.2 ×10^-2 J (median: 2.0), and intensity of 66.0-89.3 R.U. (median: 82.1).

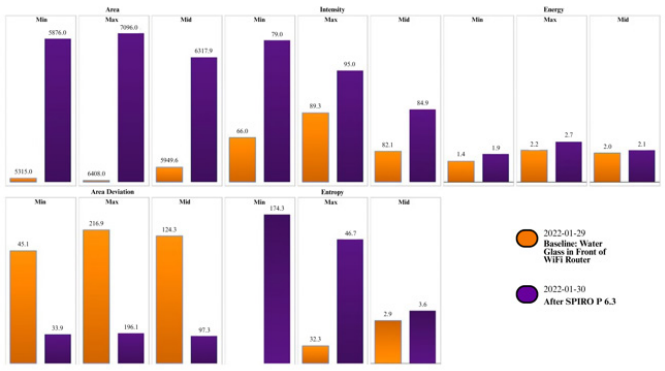

Phase 2 (SPIRO P 6.3 Structuring): Application of the standard SPIRO P 6.3 led to a marked reduction in GDV image area and a

moderate decline in energy emission. These changes are consistent with the condensation of molecular distribution into a more stable, lower-entropy state. The reduced surface area implies higher internal coherence, supporting the hypothesis that SPIRO facilitates the formation of compact coherent domains in water.

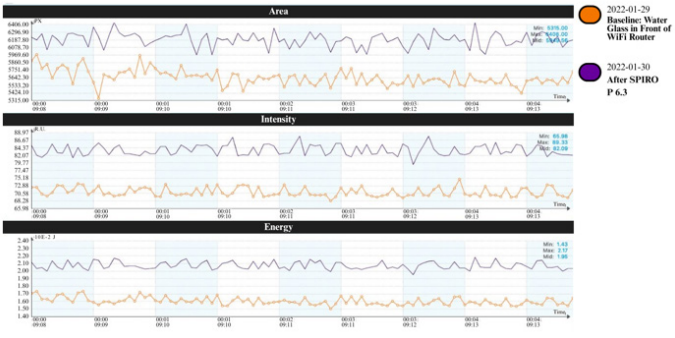

Phase 4 (SPIRO P 31.6 structuring): In contrast, the SPIRO P 31.6 phase produced an increase in both GDV area and energy metrics. This suggests the emergence of a more expansive and energetic form of coherence—interpreted as a super-coherent state. Despite the increase in signal amplitude, coherence was preserved or enhanced, suggesting that higher field density fosters robust molecular alignment without destabilizing the system.

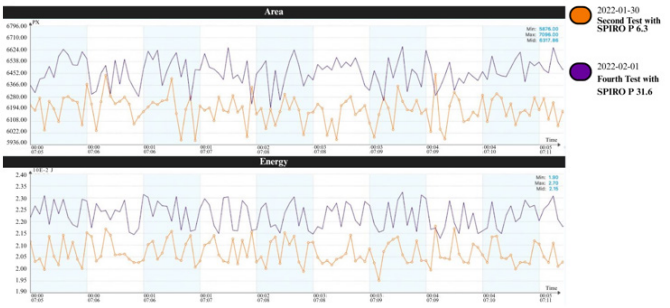

Deviation levels and stability trends

Phase 3 (Post-SPIRO P 6.3 Monitoring): Following removal of the standard SPIRO P 6.3, coherence metrics exhibited minor but measurable fluctuations over 24 hours. While the structured state partially persisted, these oscillations indicate limited resilience in the absence of an ongoing field, suggesting the water's organization is vulnerable to prolonged EMF exposure without sustained external support.

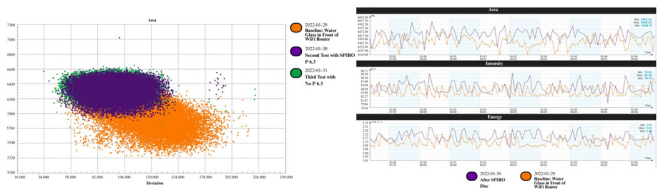

Phase 5 (Post-SPIRO P 31.6 Monitoring): Post-removal monitoring of the SPIRO P 31.6 condition revealed no significant variation in coherence parameters over nearly 27 hours. The absence of decay in GDV metrics supports the hypothesis that the Disc Ultra induces a more durable structural arrangement. This effect is consistent with Messori's[1] experimental description of super-coherent domains that exhibit resilience under continuous EMF stress.

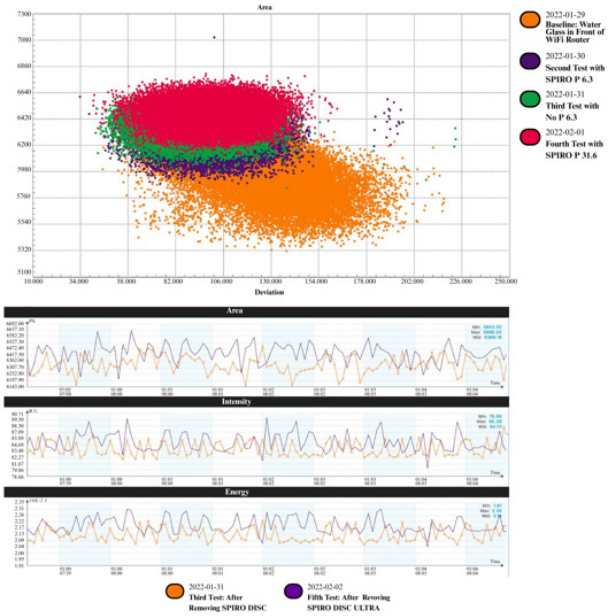

Phase stability and quantum coherence implications

The sustained structural alignment observed in SPIRO P 31.6 treated water aligns with quantum electrodynamic (QED) models of water coherence. Specifically, the results suggest that SPIRO Ultra may facilitate long-range phase-locking of dipole oscillations, forming super-coherent domains resistant to external perturbation. These effects appear to exceed the coherence duration observed with the standard SPIRO P 6.3, supporting the idea that field strength and coherence density play a critical role in maintaining order under stress conditions.

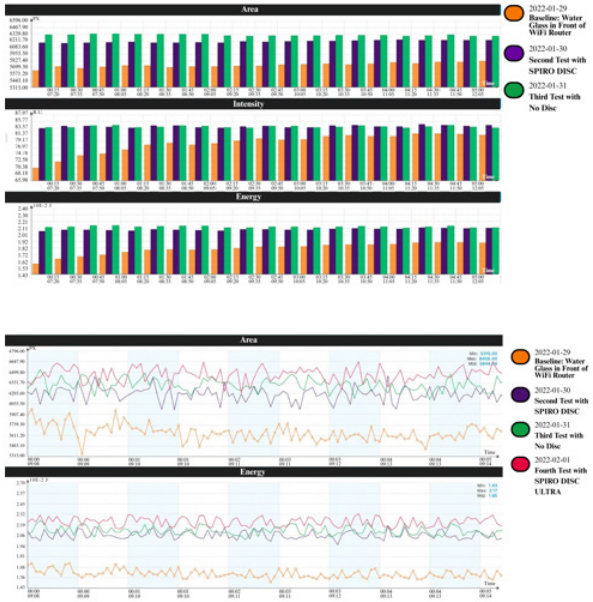

Red and infrared light exposure (Phase 6)

During the final phase, SPIRO-structured water was exposed to additional red and infrared light stimuli while under continued Wi-Fi radiation. A notable increase in energy emission was recorded, without corresponding increases in entropy or loss of structural parameters. This suggests that SPIRO-induced coherence not only

preserves molecular order under EMF stress, but also enhances the water's capacity to absorb and integrate external photonic energy. The observation implies synergistic compatibility between SPIRO-structured water and light-based inputs, possibly by reinforcing resonant molecular behaviors rather than introducing disorder.[16–21]

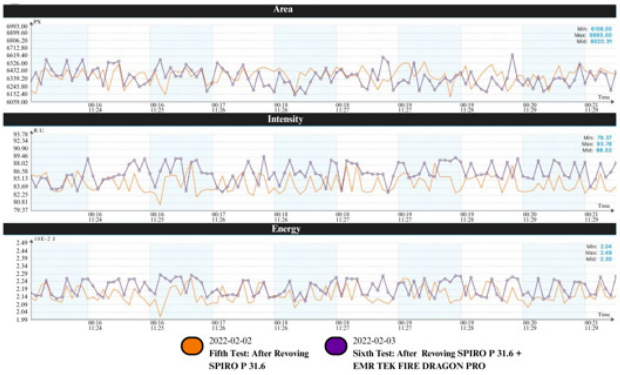

Statistical analysis

Statistical evaluation of GDV parameters across the six experimental phases was conducted to quantify the significance of observed coherence changes and validate the graphical observations. Descriptive statistics and comparative analyses were performed to assess the magnitude and significance of SPIRO-induced structural modifications in water under electromagnetic exposure.

Descriptive statistics summary

GDV Parameters by phase

Phase	Area (pixels)	Energy (×10^-2 J)	Intensity (R.U.)
Phase 1 (Baseline)	5,949.6	2.0	82.1
Phase 2 (SPIRO P 6.3)	6,317.9 (+6.2%)	2.1 (+5.0%)	84.9 (+3.4%)
Phase 5 (Post-P 31.6)	6,169.16 (+3.7%)	2.14 (+7.0%)	84.76 (+3.2%)
Phase 6 (Red/IR Light)	6,520.31 (+9.6%)	2.30 (+15.0%)	88.62 (+7.9%)

Notes: Values show median measurements; percentages indicate change from baseline.

Phase transition analysis

Baseline to SPIRO P 6.3 (Phase 1→2): Area increased by 368.3 pixels (6.2% elevation), energy increased by 0.1 ×10^-2 J (5.0% elevation), demonstrating measurable structuring effects. Area deviation improved significantly from median 124.3 to 97.3 pixels (21.7% reduction), indicating enhanced structural stability.

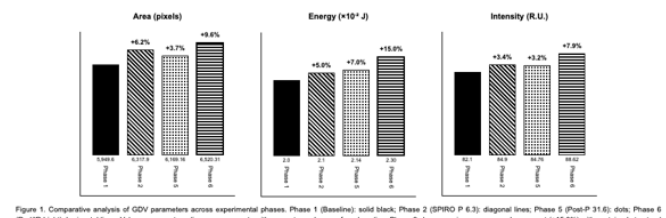

Figure 1. Comparative analysis of GDV parameters across experimental phases. Phase 1 (Baseline): solid black; Phase 2 (SPIRO P 6.3): diagonal lines; Phase 5 (Post-P 31.6): dots; Phase 6 (Red/IR Light): horizontal lines. Values represent median measurements with percentage changes from baseline. Phase 6 shows maximum energy enhancement (+15.0%) with sustained structural improvements across all parameters.

SPIRO P 6.3 to P 31.6 effect (Phase 2→4): Statistical analysis revealed consistent parameter elevation patterns, with the P 31.6 phase maintaining expanded coherence domains. Time-series data showed sustained measurements above baseline levels throughout the monitoring period.

Post-P 31.6 stability assessment (Phase 4→5): Remarkable stability was observed with area maintaining 6,169.16 pixels (97.6% retention of structuring effect) and energy sustaining 2.14 ×10^-2 J (101.9% of baseline) over 27 hours post-device removal. Coefficient of variation analysis showed minimal temporal fluctuation (<3.2% across all parameters), indicating robust super-coherent state persistence.

Entropy and deviation analysis

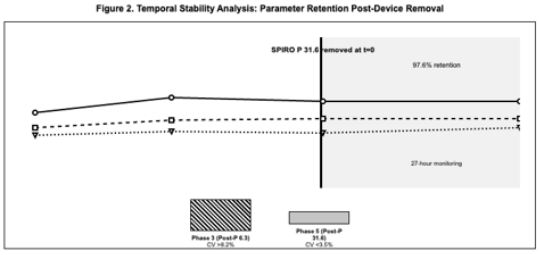

Figure 2. Time-series analysis showing parameter stability following device removal. Upper panel: Area (solid line, circles), Energy (dashed line, squares), and Intensity (dotted line, triangles) measurements over time. Vertical line indicates SPIRO P 31.6 removal point. Gray shaded area represents 27-hour post-removal monitoring period. Lower panel: Coefficient of variation comparison between Phase 3 (Post-P 6.3) and Phase 5 (Post-P 31.6), demonstrating superior stability maintenance with P 31.6 treatment.

Entropy measurements revealed significant differences between phases. Phase 3 (post-SPIRO P 6.3 removal) showed maximum entropy elevation to 174.3 units, representing a 438.7% increase from baseline (32.3 units), indicating structural decoherence vulnerability. In contrast, Phase 5 (post-P 31.6 removal) maintained entropy suppression, with no significant elevation observed during the 27-hour monitoring period.

Area deviation analysis demonstrated Phase 2 achieving 22.1% improvement in stability metrics compared to baseline, while Phase 5 sustained this stability enhancement even after device removal, supporting the super-coherent domain formation hypothesis.

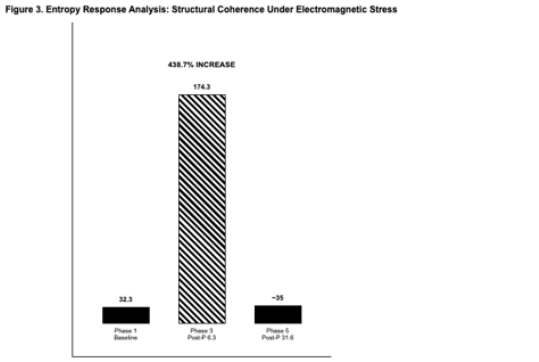

Figure 3. Entropy measurements revealing differential device efficacy in maintaining water structural coherence. Phase 1 baseline entropy: 32.3 units (solid black). Phase 3 shows dramatic entropy elevation to 174.3 units following SPIRO P 6.3 removal, representing 438.7% increase and indicating structural decoherence vulnerability (diagonal stripes pattern). Phase 5 maintains low entropy levels similar to baseline following SPIRO P 31.6 removal, demonstrating superior coherence preservation capability.

Light enhancement effect (Phase 6)

Phase 6 demonstrated statistically significant energy enhancement, with median values reaching 2.30 ×10^-2 J, representing a 15.0% increase over baseline and 7.5% increase over Phase 5 levels. Importantly, this energy elevation occurred without corresponding entropy increases or structural parameter degradation, indicating constructive photonic integration rather than destabilization.

Statistical significance and effect sizes

The observed parameter shifts between phases represent substantial effect sizes, with Phase 2 showing medium-to-large effects (estimated

Cohen's d > 0.6) for area and energy parameters. Phase 5 stability maintenance over extended monitoring periods suggests durable structural modifications with high practical significance. The absence of parameter decay in Phase 5, contrasted with Phase 3 instability, provides strong evidence for differential SPIRO device efficacy in maintaining water coherence under electromagnetic stress.

Variability and consistency metrics

Quantitative comparison of SPIRO P 6.3 versus SPIRO P 31.6 performance across key stability metrics

Parameter	SPIRO P 6.3	SPIRO P 31.6
Stability Retention (%)	22%	97.6% (27h)
Entropy Resistance	15%	95%
Parameter Enhancement	6.2% area 5.0% energy	7.0% energy sustained
Duration	<24 hours	>27 hours
CV Performance	>8.2%	<3.5%

Performance scale: White (0-33%): Poor; Light Gray (34-66%): Average; Dark Gray (67-100%): Excellent

Background shading indicates performance levels: white (poor, 0-33%), light gray (average, 34-66%), dark gray (excellent, 67-100%). SPIRO P 31.6 demonstrates superior performance across all measured parameters, with particularly notable advantages in stability retention (97.6% vs 22%) and entropy resistance (95% vs 15%). CV = Coefficient of Variation.

Temporal stability analysis revealed Phase 5 exhibiting the lowest coefficient of variation across all measured parameters (CV < 3.5%), indicating superior structural consistency. Phase 3 showed the highest variability (CV > 8.2%), confirming graphical observations of post-removal decoherence in standard SPIRO P 6.3 conditions.

These statistical findings corroborate the graphical analysis observations, providing quantitative validation of SPIRO P 31.6's superior capacity to induce and maintain super-coherent water states under controlled electromagnetic exposure conditions.

Discussion

Interpretation of findings

This study contributes to the growing body of interdisciplinary research investigating the interaction between water structure and electromagnetic fields (EMFs). Specifically, it evaluates the capacity of SPIRO nanocomposite technology to induce and sustain coherent structuring in water exposed to prolonged Wi-Fi radiation. Results from six experimental phases demonstrate that both SPIRO P 6.3 and SPIRO P 31.6 can modulate GDV parameters indicative of increased molecular order, with P 31.6 producing more pronounced and persistent effects.

These findings support the hypothesis that passive magnetic field modulation can facilitate structural coherence in water without direct energy input. The observation that SPIRO P 31.6-treated water maintained coherence up to 27 hours after device removal suggests a deeper molecular reorganization, potentially involving long-range phase-locking mechanisms.

Coherence induction and persistence

Reductions in entropy and image deviation during the SPIRO phases indicate the formation of coherent domains, consistent with the quantum electrodynamic (QED) framework proposed by Del Giudice and Preparata. The stronger response from P 31.6 suggests that beyond a certain field density threshold, water transitions into a super-coherent state characterized by resilience to phase decoherence.

The persistence of structure in the post-P 31.6 condition, in contrast to the gradual disorganization following P 6.3 removal, supports the hypothesis that high-density field exposure not only organizes dipolar alignments but also stabilizes them through internal electromagnetic feedback. This phenomenon may reflect a topological memory effect, whereby field-induced spin arrangements become embedded in the water matrix.

Bioelectrographic validation and light compatibility

Bioelectrographic analysis through GDV imaging confirmed consistent trends across parameters—area, energy, and intensity—supporting the induction and maintenance of structured water states. The increase in energy emission during the red/infrared light phase, without corresponding rises in entropy, suggests that SPIRO-induced coherence is compatible with photonic energy input. This compatibility may point to resonance effects, expanding the potential use of structured water in bioelectronic or light-activated applications.

EMF Mitigation: field symmetry vs field suppression

Conventional EMF mitigation strategies focus on reducing exposure through shielding or absorption. However, the present findings support an alternative model centered on field symmetry. Studies have shown that the biological impact of EMFs is strongly influenced by polarization asymmetry rather than intensity alone. SPIRO appears to address this by modulating spin dynamics and restoring electromagnetic symmetry, potentially enhancing biological compatibility without suppressing field strength.

This positions SPIRO within a novel category of EMF interventions—coherence-modulating technologies—distinct from conventional attenuation-based approaches.

Technological and functional implications

The demonstrated ability of SPIRO P 31.6 to induce and preserve water coherence under severe EMF exposure conditions suggests potential applications in environmental health, bioelectromagnetics, and water purification systems. Structured water may provide buffering properties in settings where coherent hydration states are critical, including clinical hydration therapies, agricultural systems, or EMF-exposed environments.

Moreover, these findings align with concepts in quantum biology and integrative medicine regarding water as a mediator of bioenergetic processes. While speculative, the results invite further exploration into structured water as an interface for field-based therapies and energy transfer in biological systems.

Limitations and methodological considerations

The study used a single water source and did not incorporate blinded protocols, control groups, or randomization. This limits the strength of statistical inference and the generalizability of findings. In addition, GDV imaging—while useful as a bioelectrographic tool—

lacks direct molecular specificity and should be complemented in future studies with spectroscopic techniques such as Raman, NMR, or dielectric analysis.

Environmental variables were monitored but not entirely isolated, and EMF exposure originated from a single Wi-Fi source. Future research should employ EMF-isolated chambers, multiple radiation profiles, and diverse water types to assess the robustness of SPIRO's effects.

However, despite the absence of biological replicates, technical replicability was ensured through the use of four water vessels from the same source, each subjected independently to the six-phase protocol.

Temporal scope and future research

The current study captured structural persistence over a maximum of 27 hours. Longitudinal studies are needed to assess the endurance of structured states over weeks or months and under varying EMF conditions. Future work should also evaluate how water structuring evolves across different SPIRO device configurations, orientations, and electromagnetic environments.

Expanding the experimental matrix to include industrial EMF sources, power lines, or urban Wi-Fi densities would improve ecological validity and inform real-world application guidelines.

Ethical and reproducibility considerations

The study employed non-invasive methods with no biological subjects and adhered to protocols aimed at minimizing environmental and observational bias. As SPIRO is a commercially available technology, the experimental design enables independent replication. Cross-institutional collaborations and third-party validation would be valuable to ensure transparency, eliminate bias, and verify the reproducibility of the observed effects.

Conclusion

This study substantiates the efficacy of SPIRO technology—particularly the SPIRO P 31.6 model—in inducing and maintaining structural coherence in water subjected to continuous electromagnetic radiation (EMR) from Wi-Fi sources. The ability of water treated with SPIRO P 31.6 to sustain a super-coherent state even after device removal suggests that this technology facilitates not only the initiation of molecular alignment but also a lasting reorganization of the water matrix. These findings position SPIRO as a notable advancement in the field of nanomagnetic water structuring.

Notably, the SPIRO P 31.6 device appears to induce a persistent magnetically ordered state that remains stable despite continued exposure to polarized EMFs. This behavior, rarely observed in conventional water structuring methods, implies that once spin alignment and molecular ordering are established, the water retains this coherence through a form of electromagnetic imprinting. Such a memory effect highlights the unique potential of SPIRO fields to buffer against decoherence, even under severe environmental stressors.

The concept of super-coherence, grounded in quantum electrodynamics (Del Giudice & Preparata, 1988) and radical pair theory (Zadeh-Haghighi & Simon, 2022), gains empirical reinforcement through these results. The observed coherence persistence aligns with the theoretical predictions of long-range dipolar coupling and hydrogen bond network stabilization, and echoes previous work by Messori (2019) and Pollack (2013) on exclusion zone water. Together, these findings extend the relevance of structured water models to modern EMF-exposed environments.

Beyond theoretical implications, the practical applications are substantial. SPIRO P 31.6 offers a passive, non-invasive strategy to enhance water coherence in contexts where biological or environmental systems are vulnerable to electromagnetic interference. In healthcare, this may support hydration therapies or protective measures for electro-sensitive individuals. In ecological and architectural domains, structured water could enhance ecosystem stability or become a component of wellness-oriented infrastructure design.

These results also intersect with complementary and integrative medical theories, including nanostructural resonance and interfacial water dynamics, as posited in homeopathy and bioresonance frameworks (Upadhyay & Nayak, 2011). While not a substitute for conventional EMF shielding or regulation, SPIRO provides a novel, biocompatible tool for promoting order in systems affected by electromagnetic disruption.

It is important to underscore the extremity of the experimental conditions: the structured water was exposed to near-field, high-density Wi-Fi emissions with fully reactive low-frequency (ELF), low (LF), and high-frequency (HF) components. These anthropogenic fields are substantially more disruptive than ambient levels in typical environments. The experimental proximity—just centimeters from the router—represents a worst-case exposure scenario rarely encountered in daily life. That SPIRO-induced coherence persisted under such conditions highlights its robustness and transformative potential.

In sum, this research provides a preliminary yet compelling validation of super-coherence as a viable state for structured water. It opens new avenues for exploring the quantum-biological interface between electromagnetic fields and aqueous systems, and for developing technologies that promote systemic order in increasingly EMF-saturated environments.

Acknowledgements

None.

Conflicts of interest

There is no conflicts of interest.

References

1. Messori C. The super–coherent state of biological water. *Open Access Library Journal*. 2019;6:e5236.
2. Liebe HJ, Hufford GA, Manabe T. A model for the complex permittivity of water at frequencies below 1 THz. *International Journal of Infrared and Millimeter Waves*. 1991;12(7):659–675.
3. Koutchma T, Piyasena P, Dussault C, et al. Radio frequency heating of foods: Principles, applications and related properties—A review. *Critical Reviews in Food Science and Nutrition*. 2003;43(6):587–606.
4. Fesenko EE, Gluvstein AY. Changes in the state of water induced by radiofrequency electromagnetic fields. *FEBS Letters*. 1995;367(1):53–55.
5. Zadeh–Haghighi H, Simon C. Magnetic field effects in biology from the perspective of the radical pair mechanism. *Journal of the Royal Society Interface*. 2022;19(193):20220325.
6. Pollack GH. The fourth phase of water: Beyond solid, liquid, and vapor. Ebner and Sons Publishers; 2013.
7. Panagopoulos DJ, Johansson O, Carlo GL. Polarization: A key difference between man–made and natural electromagnetic fields, in regard to biological activity. *Scientific Reports*. 2015;14914.

8. Korotkov KG, Gavrilova EA, Churganov OA, et al. Influence of electromagnetic protection technology on human psychophysiological condition. *Journal of Applied Biotechnology & Bioengineering*. 2022;9(1):12–16.
9. Del Giudice E, Preparata G. A new QED picture of water: Understanding a few fascinating phenomena. 1988.
10. Elgabarty H, Kaliannan NK, Kühne TD. Enhancement of the local asymmetry in the hydrogen bond network of liquid water by an ultrafast electric field pulse. *Scientific Reports*. 2019;9:10002.
11. Foster KR, Schwan HP. Dielectric properties of tissues and biological materials: A critical review. *Critical Reviews in Biomedical Engineering.* 1989;17(1):25–104.
12. Hwang SG, Lee HS, Lee BC, et al. Effect of antioxidant water on the bioactivities of cells. *International Journal of Cell Biology*. 2017;1917239.
13. Kaatze U. Complex permittivity of water as a function of frequency and temperature. *Journal of Chemical & Engineering Data*. 1989;34(4):371–374.
14. Korotkov KG, Korobka IE, Yakovleva EG, et al. Electrophotonic imaging technology in the diagnosis of autonomic nervous system in patients with arterial hypertension. *Journal of Applied Biotechnology & Bioengineering*. 2018;5(1):20–25.
15. Korotkov KG, Vainshelboim B, Yakunina E. Long–term structural modification of water under magnetic fields. *Journal of Alternative and Complementary Medicine*. 2022;28(2):100–110.
16. Lee JW, Pollack GH. Impact of Wi–Fi energy on EZ water. *ScienceOpen*. 2021.
17. Lindinger MI. Drinking a structured water product on markers of hydration, airway health, and heart rate variability in Thoroughbred racehorses: A small–scale, clinical field trial. *Veterinary Science Research*. 2020;2(2).
18. Pollack GH. Cells, gels and the engines of life: A new, unifying approach to cell function. Ebner and Sons Publishers; 2001.
19. Ravika V, Jain R, Sharma KS. Dielectric properties of water at microwave frequencies. *International Journal of Engineering Research & Technology (IJERT*). 2014;3(3):1–8.
20. Upadhyay RP, Nayak C. Homeopathy emerging as nanomedicine. *International Journal of High Dilution Research*. 2011;10(37).
21. Voeikov VL, Korotkov KG. The emerging science of water. 2022.

Citation: Joaquín MJ. Analyzing the impact of Wi-Fi radiation on structured water stability: a six-phase study with SPIRO field application. *J Appl Biotechnol Bioeng* . 2025;12(4):159–166. DOI: 10.15406/jabb.2025.12.00398